university of groningen / faculty of science and engineering

University of Groningen, Groningen

Bachelor Research Project

Faculty of science and engineering

Understanding host-guest interaction of trimesic acid in a porous molecular network

Student:
Jeanne van Zuilen
S3133516

Daily supervisor:
Dr. M. Enache
First examiner:
Prof. Dr. M. A. Stöhr
Second examiner:
Prof. Dr. L.J.A. Koster

July 2020

Abstract

In this research the host-guest network of 3-deh-DPDI and trimesic acid (TMA) on a Cu(111) surface is studied. 3-deh-DPDI is the deprotonated form of 4,9-diaminoperyline-quinone-3,10,diimine (DPDI) where the nitrogen atoms form double bonds with one another. The 3-deh-DPDI network is a self-assembled network (SAN) that acts as a host for the TMA molecules. The goal of the research was to understand the host-guest interactions of this network. To achieve this, scanning tunneling microscope (STM) images of the network are analysed. The images were obtained under ultra high vacuum (UHV) conditions. The unit cell of the network has lattice parameters $a = 2.3\ nm, b = 2.2\ nm$ *and* $\theta = 57°$. For a low TMA coverage it is found that the TMA molecules prefer to sit alone inside a pore. For higher TMA coverages the TMA molecules do not show a clear preference. It is found that the TMA molecules sit lower inside the pore after annealing at 150 °C. Furthermore, molecular models that describe how the TMA molecules sit inside the pores of the network are proposed. In the proposed models the TMA molecules are fully deprotonated and coordinate together with Cu adatoms that have diffused from the step edges of the surface.

Contents

1 Introduction

In 1987, the Nobel Prize for Chemistry was awarded to *Cram, Lehn and Pedersen* for their development and application of molecules with selective structure specific interaction. This laid the foundation for an interdisciplinary area of research that is now known as *supramolecular chemistry* [1]. An important field in supramolecular chemistry is the self-assembly of molecules. Self-assembly is described as the assembly of molecules without guidance or management from an outside source [2, 3]. When the correct substrate and molecule are chosen the molecules can self-assemble into a monolayer or self-assembled network (SAN) on the surface. The organization of a SAN is the result of noncovalent interactions between the molecules. Self-assembly is believed to open up the possibility to molecular electronics, the successor of today's electronics which are based on silicon technology [4]. Under the right conditions (such as substrate, solution and temperature) it is possible for molecules to self-assemble into a porous network. Such a porous network might be able to host guest molecules inside its pores, which is then called a host network. A solid surface underneath the network ensures a high degree of crystallinity and provides additional stability to the host-guest network via molecule-surface interactions. The controlled hosting of guests inside the pores offers the opportunity to applications like separation technology and molecular sensing [5]. These molecular networks can be studied using a scanning tunneling microscope (STM). This microscope is able to image the surface of the sample by scanning its conductive tip parallel to the surface using piezo elements. By applying a bias voltage and scanning close enough to the surface a tunneling current is induced. This tunneling current is exponentially dependent on the distance between the tip and sample and can therefore be used to map the topography of the sample.
The aim of this research is to understand how the guest molecule (trimesic acid) interacts with its host network (3-deh-DPDI) on a Cu(111) surface. The 3-deh-DPDI network is a self-assembled network. This was done by analyzing STM images that were obtained by *M. Enache*. The network that was imaged has a porous structure in whose pores trimesics acid (TMA) is hosted. The TMA molecules arrange with either one, two or three TMA molecule(s) inside the pores of the network. In order to understand the host-guest interaction the unit cell of the network is determined(), the occurrence of the TMA molecules inside the pores is investigated, the differences that resulted from annealing the network are compared and a proposal on the molecular model that can explain how the TMA molecules sit inside the pores of the network is given.

2 Theoretical background

2.1 Scanning tunneling microscopy

The scanning tunneling microscope is an instrument that can image the surface of a conductive sample with atomic resolution. This is done by scanning a conductive tip parallel to the surface, with a distance between tip and sample of approximately 1 nm, so that a tunneling current between the tip and sample can occur. The height of the sample is recorded at every point, so that a so-called topographic image can be made. A schematic of the STM is depicted in figure 1.

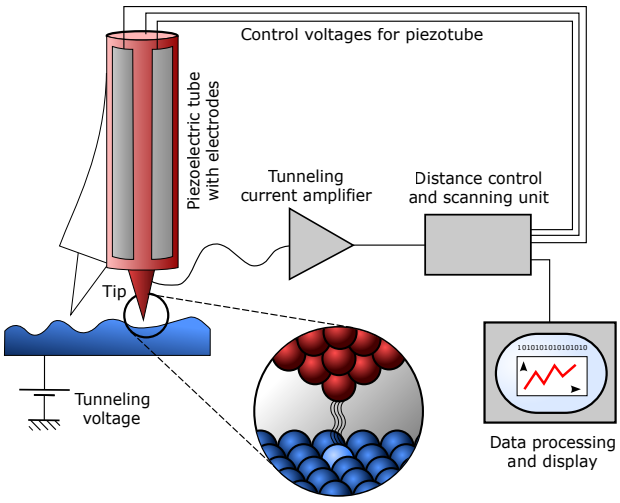

Figure 1: *Schematic of a scanning tunneling microscope. Adapted from [6].*

The tip, usually made of tungsten (W) or platinum-iridium (Pt-Ir), is scanned over the sample with the use of a piezoelectric tube. The piezo elements in the tube expand or contract depending on the magnitude and sign of the applied voltage. The tip is brought within nanometer range of the sample so that the electron wavefunctions of the tip and sample overlap, enabling tunneling. By applying a bias voltage between the tip and sample a directed tunneling current is generated. If the tip is grounded and the bias voltage is applied to the sample, we speak of a *sample voltage*. When $V > 0$, the electrons tunnel from the occupied states of the tip into the empty states of the sample. Whereas if $V < 0$, the electrons tunnel from the occupied states of the sample into the empty states of the tip. The magnitude of the tunneling current depends on the applied voltage and the overlap of the local density of states of both the tip and sample. The tunneling current is exponentially dependent on the distance between tip and sample (equation 1) where I is the tunneling current, V is the bias voltage, d is the distance between tip and sample and k is a proportionality constant. [7]

$$I \propto Ve^{-kd} \tag{1}$$

The STM can be operated in two modes, *constant current mode* and *constant height mode*. In constant height mode the tip of the STM is kept at a constant height by keeping the voltage at the z piezo constant, and the current is recorded. Because the tunneling current is exponentially dependent on the distance between tip and sample, the height profile can be found from the current profile recorded. In constant current mode the current is kept constant with the use of a feedback loop that regulates the tip height. The topography of the sample is obtained from recording the **z** signal of the tip. Constant height mode is able to scan quicker than constant current mode because no feedback loop is necessary. However, it comes with the risk of crashing into the sample because there is no feedback loop that raises the tip if there is a bump in the sample. To reduce the risk, one can use the slower constant current mode.

2.2 Molecular self-assembly on surfaces

Molecular self-assembly is the assembly of molecules without guidance or management from an outside source [2, 3]. Molecular self-assembly on surfaces can result in self-assembled monolayers (SAMs) when the molecule and substrate are chosen correctly. Some examples of SAMs that were fabricated under ultra high vacuum (UHV) conditions are 1,3,5-benzenetribenzoic acid (BTB) on both Cu(111) and epitaxial graphene grown on Cu(111)[8] or TMA on Cu(100)[9] and Cu(110)[10]. The organization of the well-ordered networks is a result of noncovalent interactions between the moleluces, such as hydrogen bonding, van der Waals interactions or metal-ligand coordination. The physical shape of the molecules and the directionality of the bonds involved will influence the geometry of the SAMs. Furthermore, the balance between molecule-surface interaction, intermolecular interactions and parameters like temperature and deposition rate influence the final geometry of the network as well [4, 11].

It is possible that the molecules assemble in a porous network. An important application of two-dimensional nanoporous networks is the hosting of guest molecules inside the pores of the network. Host-guest chemistry describes the formation of structural complexes which consist of two or more molecules or ions via noncovalent interactions [5]. Often the host network is self-assembled on a surface that ensures a high degree of crystallinity. The presence of a solid surface not only ensures a high degree of crystallinity in the host network, thus enabling an efficient capture of guests, but it also provides additional stability to the host–guest network via molecule–surface interactions. The network is sustained by noncovalent interactions between the molecules. A host network that is formed at the solid-liquid interface can also be stabilized by co-adsorption of solvent molecules. When the size and shape of the guest molecule matches the size and shape of the pores, the guest molecule can be immobilized on the surface within the pores of the host network. The stabilization of the guest occurs via interactions with the host network as well as with the surface. Thus the host-guest chemistry on surfaces is surface assisted [5]. An example of a host-guest network is depicted in figure 2. Here a chickenwire network of TMA is able to host buckyballs (C60) inside its pores. The buckyballs show up as bright protrusions on the STM image, in the top left and bottom right corners. This was done under ambient conditions by *S. Griessl et al.* [12].

In order to visually simplify the crystalline patterns solids arange themselves in, one can use a unit cell. An ideal crystal consists of an infinite repetition of identical groups of atoms in three dimensions. The smallest repeating group of atoms in the repeating pattern is called the basis. When this basis is placed on a single set of lattice vectors it forms the unit cell. When the unit cell is repeated an infinite amount of times it forms the crystal structure [13]. The unit cell is generally depicted by a parallelogram with sides a and b, and an angle between a and b of θ, where the sides have the length of the lattice vectors. A schematic of a unit cell can be found in figure 3.

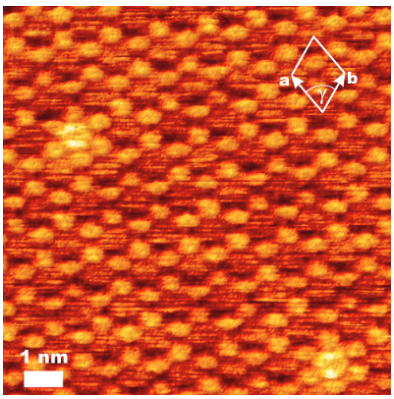

Figure 2: *STM image of a TMA network that acts as a host for buckyballs under ambient conditions on a graphite surface. The buckyballs show up as bright protrusions on the image. Adapted from the work of Griessl et al. [12]. (10 nm x 10 nm, $a = b = 1.6 \pm 0.1$ and $\gamma = 60 \pm 1^{\circ}$)*

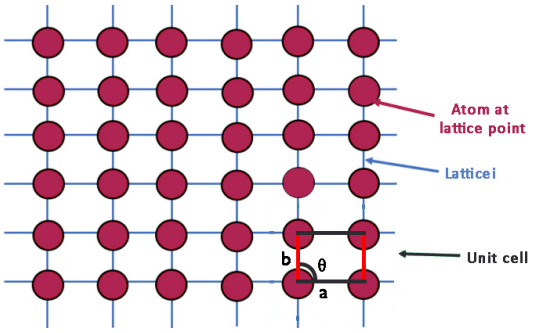

Figure 3: *Schematic representation of a unit cell. The vectors a and b are the lattice vectors and the parallelogram that is enclosed by the vectors is the unit cell.*

2.3 DPDI and 3-deh-DPDI

DPDI, or 4,9-diaminoperylene-quinone-3,10-diimine (figure 4, left), consists of a perylene core to which at each end an NH and NH_2 group are attached. When DPDI is deposited onto a Cu(111) surface with submonolayer coverage at room temperature under UHV conditions the molecules are found to be mobile, forming no ordered structure. Upon annealing at 200°C, the DPDI molecules undergo a chemical transformation: the nitrogen atoms of DPDI are deprotonated and a double bond between the nitrogen atoms is formed, resulting in 3-deh-DPDI (figure 4, right) [14]. In the annealing process Cu adatoms diffuse from the step edges of the surface, which then coordinate to the nitrogen atoms of three adjacent 3-deh-DPDI molecules. This results in a 2 dimensional metal-organic framework (2D MOF), depicted in figure 5, that is centered around a hollow site of the Cu surface and has a threefold rotational symmetry. As a result of the adatom-nitrogen coordination, the molecule-substrate interaction is decreased and the molecules are almost decoupled from the Cu surface [14]. This 2D MOF is stable up to 300°C, and is commensurate with the Cu(111) surface in a $p(10 \text{ x } 10)$ manner [15]. Because the network is stable and porous, the pores can be used to host guest molecules such as TMA.

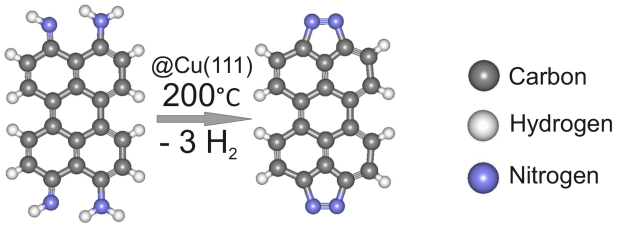

Figure 4: *The molecular models of DPDI (left) and its deprotonated form: 3-deh-DPDI (right).*

2.4 Trimesic acid

Trimesic acid, or benzene-1,3,5-tricarboxyl acid, consists of a benzene ring to which three carboxylic acid groups are attached. A molecular model of TMA is depicted in figure 6. Because of the carboxyl groups, TMA can coordinate with other TMA molecules and form stable supramolecular networks. Two examples of these networks are the chickenwire structure and the flower structure at the interface between nonanoic acid/highly oriented pyrolytic grapite (HOPG) from the work by *Ubink et al.*, depicted in figure 7 [16]. In the chickenwire structure the TMA molecules assemble with only dimeric hydrogen bonds. In the flower structure the TMA molecules assemble with both dimeric and trimeric hydrogen bonds, leaving a more densely packed porous structure. The dimeric hydrogen bonds are double bonds, whereas the trimeric bonds are single hydrogen bonds.
Furthermore, a TMA molecule can bind to its neighbours in three different motifs, *tip-to-tip*, *tip-to-side* and *side-to-side*. The three different motifs are depicted in figure 8a, together with an STM image from *Classen et*

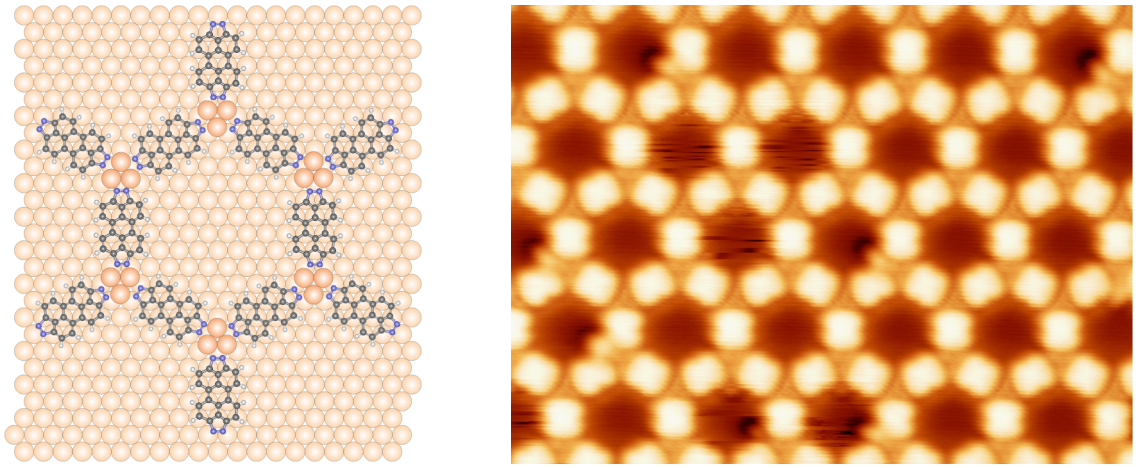

(a) *(b)*

Figure 5: *Metal organic framework of 3-deh-DPDI on Cu(111). Figure 5a depicts the schematic model of the 3-deh-DPDI network on Cu(111). Figure 5b depicts an STM image of the 3-deh-DPDI network on a Cu(111) surface. The DPDI coverage is 0.66 Å. (12.2nm x 9.4nm, U = 0.3 V).*

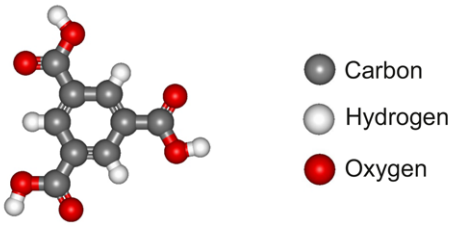

Figure 6: *Molecular model of trimesic acid.*

al. showing the three different motifs in figure 8b [10]. The motifs were found on a Cu(110) surface under UHV conditions. It was noted by *Classen et al.* that the motifs are also possible for partially deprotonated TMA molecules.

The carboxyl groups of TMA are known to potentially deprotonate on Cu surfaces. In a study from *N. Lin et al.* it was found that the deprotonation of TMA was accelerated by the addition of Cu adatoms on a Ag(111) surface, suggesting that the deprotonation of TMA is due to Cu adatoms [17]. The full deprotonation of TMA and coordination with Cu adatoms on a Cu(100) at room temperature was found by *N. Lin et al.* years earlier [18]. In the study by *Classen et al.*, mentioned above, the adsorption of TMA on Cu(110) under UHV conditions was studied in the temperature range between 130 and 550 K. It was found that for temperatures up to 280 K the TMA molecules were partially deprotonated and for temperatures above this threshold the molecules were fully deprotonated. When fully deprotonated, the molecules formed metal-organic structures together with the Cu adatoms that had diffused from the step edges [10].

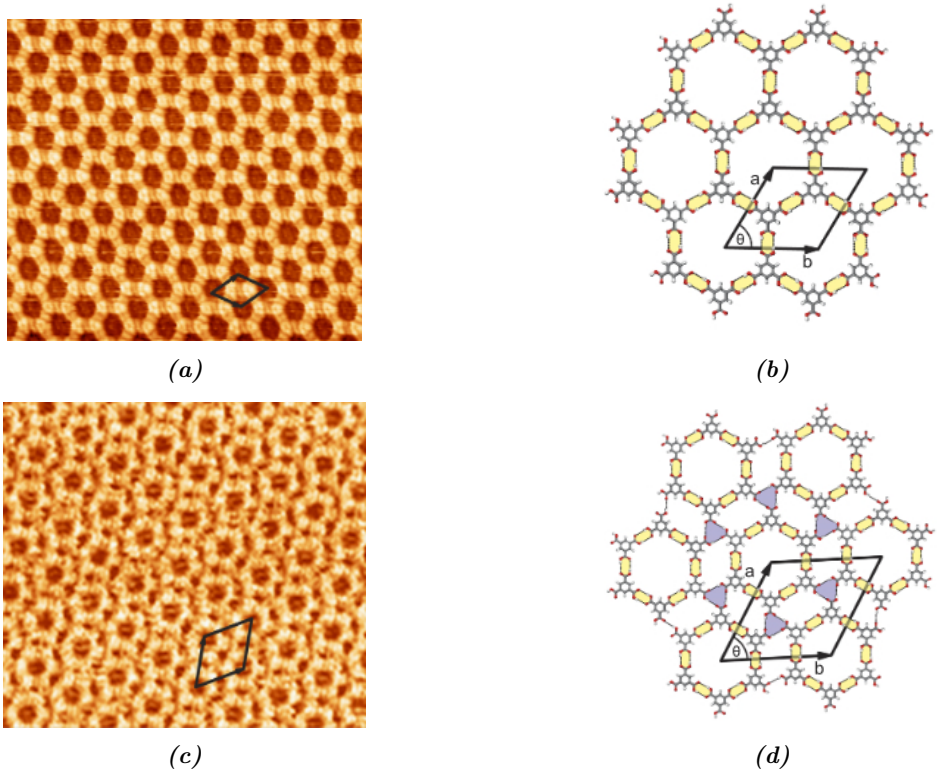

(a) *(b)*

(c) *(d)*

Figure 7: *STM images and molecular models of the chickenwire and the flower structure formed by TMA at the interface between nonanoic acid and HOPG. Unit cells are depicted in black. Figure 7a shows an STM image of the chickenwire structure (20 nm x 20 nm, U = -1 V). Figure 7b shows the molecular model of the chickenwire structure. Unit cell parameters: a = b = 1.6 nm and θ = 60°. Figure 7c shows an STM image of the flower structure (20 nm x 20 nm, U = 0.5 V). Figure 7d shows the molecular model of the flower structure. Unit cell parameters: a = b = 2.5 nm and θ = 60°. All figures are adapted from [16].*

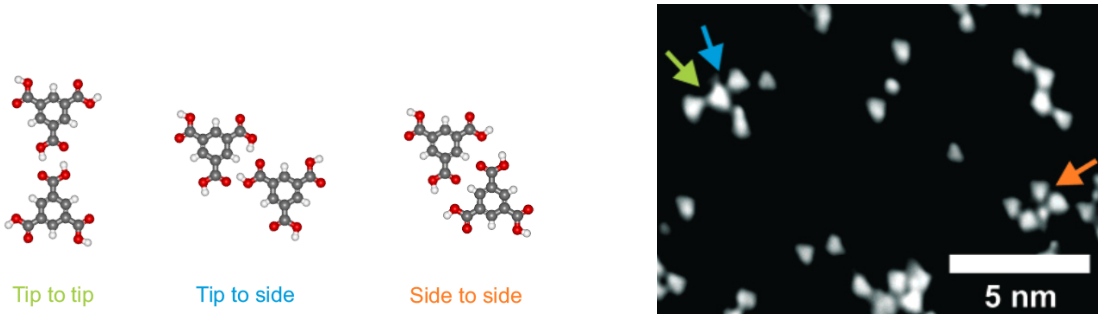

(a) *(b)*

Figure 8: *Representation of three motifs in which neighbouring TMA molecules can coordinate, together with an STM image that represents every motif. Figure 8a shows the three different motifs proposed by Classen et al. for neighbouring TMA molecules. Figure 8b shows an STM image from the work by Classen et al. where the three different motifs can be seen under UHV conditions on a Cu(110) surface[10].*

3 Experimental background

The STM images used in this research were obtained by *M. Enache* and were acquired at 77 K under UHV conditions. DPDI molecules were deposited on a Cu(111) surface in order to obtain the porous host network, for three different coverages. After obtaining the network, TMA molecules are deposited onto the sample at room temperature. The first sample has a DPDI coverage of 0.6 $\dot{A}$, and a TMA coverage of 0.3 $\dot{A}$. This sample was imaged before and after annealing at 150 °C. The second sample has a DPDI coverage of 1 $\dot{A}$ and TMA was gradually added from 0.1 $\dot{A}$ to 0.5 $\dot{A}$, where images were taken after every increase of TMA coverage. In the third sample there was a DPDI coverage of 1.44 $\dot{A}$ and a TMA coverage of 0.13 $\dot{A}$ and 0.53 $\dot{A}$. A summary of the samples and their DPDI and TMA coverages is given in table 1. The images were processed with the use of WSxM [19] and scaling of images and determination of the molecular model was done with the use of CorelDraw. To see if there is a correlation between the coverage and the number of TMA molecules that like to arrange in a single pore, the occurrence of every set was counted for non-duplicate STM images.

Sample number	DPDI coverage ($\dot{A}$)	TMA coverage ($\dot{A}$)	Notes
I	0.6	0.3	Imaged before and after annealing at 150 °C
II	1	0.1 - 0.2 - 0.3 - 0.5	
III	1.44	0.13 - 0.53	

Table 1: *Summary of the different samples that were investigated.*

4 Results and discussion

The 3-deh-DPDI network is able to host TMA molecules inside its pores. The TMA molecules arrange themselves with either one, two or three molecules inside a pore. An example of each arrangement can be seen in figure 9.

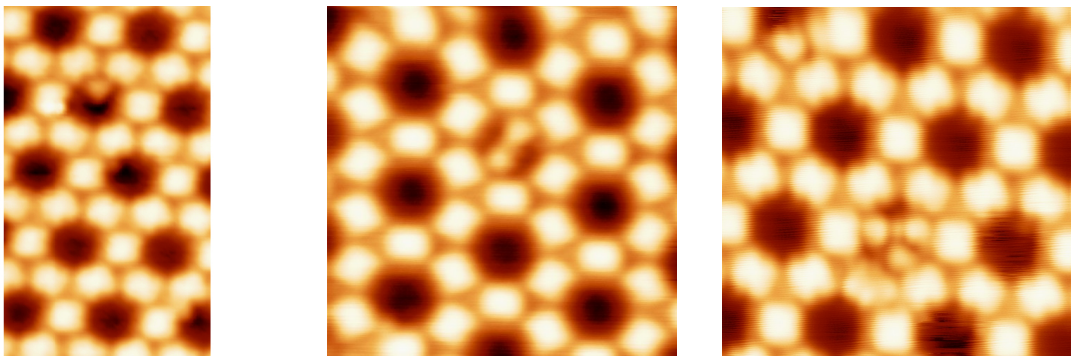

(a) ***(b)*** ***(c)***

Figure 9: *STM images of TMA in the 3-deh-DPDI network.There is either one, two or three TMA molecule(s) inside a pore. All images were taken before annealing and with a DPDI coverage of 0.6 $\dot{A}$ and a TMA coverage of 0.3 $\dot{A}$. Figure 9a shows a single TMA molecule inside a pore ($U = 1.5V$, 6.7 nm x 10.6 nm). Figure 9b shows two TMA molecules inside a pore ($U = -1.5V$, 7 nm x 7 nm). Figure 9c shows three TMA molecules inside a pore ($U = 1.3V$, 7 nm x 7 nm).*

4.1 Unit cell of the 3-deh-DPDI network

The unit cell of the network was determined by determining the parameters for every image and taking the average over all images. The determined unit cell has parameters, $a = 2.3 \pm 0.2$ nm, $b = 2.2 \pm 0.2$ nm and $\theta = 57 \pm 5°$. This is not in accordance with the unit cell determined by *Matena et al.* [14]. The unit cell determined by *Matena et al.* has lattice constants $a = b = 2.55$ nm and $\theta = 60°$. Their unit cell is determined with higher precision, as their unit cell was determined with the use of low-energy electron diffraction (LEED) instead off STM images as done in this research. In LEED experiments a beam of low energy electrons bombard a surface. The electrons are diffracted by the surface structure enabling the structure to be deduced [20]. The angle of the determined unit cell falls within the error bounds, however the lattice constants do not. This is likely a result of incorrect calibration of the STM. The determined unit cell and the unit cell determined by *Matena et al.* are depicted in figure 10.

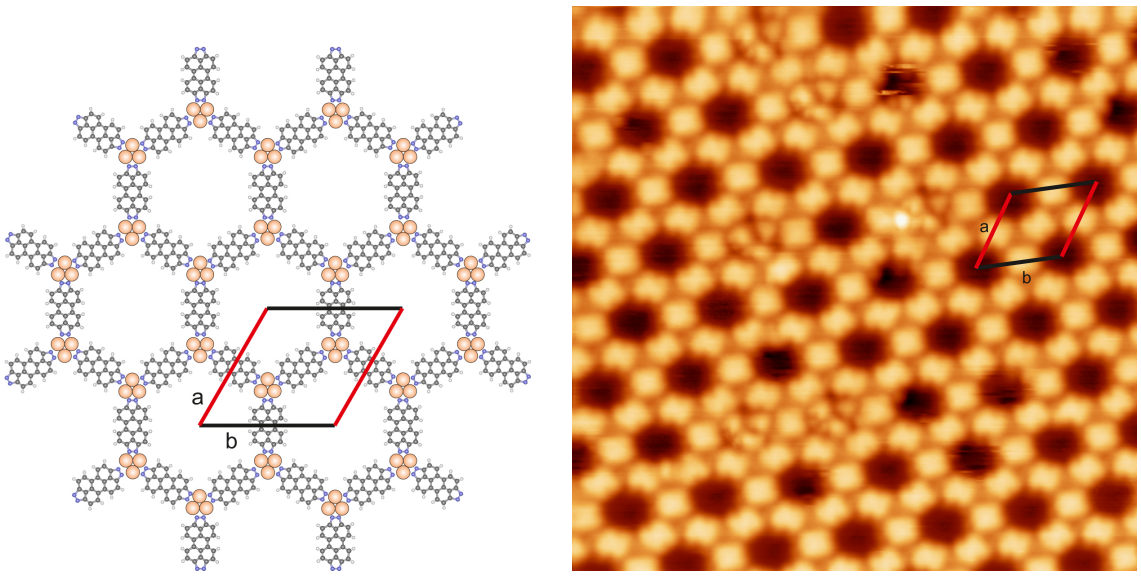

(a) *(b)*

Figure 10: *A schematic model of the 3-deh-DPDI network and an STM image of the network. Figure 10a shows the unit cell on the schematic model, with lattice parameters:* $a = b = 2.55$ *nm and* $\theta = 60°$*. Figure 10b shows the determined unit cell depicted on an STM image with lattice parameters:* $a = 2.3$ *nm,* $b = 2.2$ *nm and* $\theta = 57°$ *(15 nm x 15 nm,* $U = 1.3$ *V).*

4.2 Statistics on TMA occupancy

In figure 11, the statistics on the occupancy of TMA inside the pores are depicted. For the first sample (figure 11a), it can be seen that TMA prefers to sit with three molecules inside the pore, both before and after annealing. However this preference changes slightly. The preference for three molecules inside a pore increases after annealing. From the second sample (figure 11b) it can be seen that for a TMA coverage of 0.1 $\dot{A}$ there is a preference for the TMA molecules to sit alone inside a pore. With increasing coverage, this preference reduces and the TMA molecules do not show a strong preference for any specific number of molecules in one pore anymore. For the third sample (figure 11c) it can be seen that for a low TMA coverage (0.13 $\dot{A}$) there is a strong preference for the TMA molecules to sit alone in a pore. When the coverage is increased to 0.53 $\dot{A}$, this changes to a strong preference for two molecules inside a pore.
To see if the preferences change with TMA coverage, the TMA occurrence as function of the TMA coverage is plotted in figure 12. This is done for TMA coverages of 0.1(3), 0.3 and 0.5(3) $\dot{A}$. In figure 12a it can be seen that for both a DPDI coverage of 1 $\dot{A}$ and 1.44 $\dot{A}$ the TMA molecules have a strong preference to sit alone inside a pore. With an increased TMA coverage (figure 12c) this preference disappears for a DPDI coverage of 1 $\dot{A}$ and changes from one inside a pore to two inside a pore for a DPDI coverage of 1.44 $\dot{A}$. In figure 12b it can be seen that for a DPDI coverage of 0.6 $\dot{A}$ the TMA molecules have a strong preference to sit with three inside a pore. For a DPDI coverage of 1 $\dot{A}$ the TMA molecules show no preference. Because there are only two data points per TMA coverage no clear relation between the preferences of the TMA molecules and the DPDI coverage can be determined.
It was not tested if the distribution of the TMA molecules over the pores is purely statistical. A possible way of doing this is by counting the total amount of pores, so empty ones and ones that host TMA. The probability that one TMA lands inside a pore is $1/\ number\ of\ pores$. It does not matter if the pore is already filled or if it is empty. This means that the probability of having two TMA molecules inside the pore is $(1/\ number\ of\ pores)^2$ and $(1/\ number\ of\ pores)^3$ for three TMA molecules inside a pore. Thus the probability of finding two or three molecules inside a pore is lower than for one TMA molecule. From the first dataset (figure 11a) it can be observed that this is not the case for this network. An explanation for this could be that that there are interactions between the TMA molecules. Furthermore, it is noticed that the TMA molecules have a slight preference to assemble around defects of the 3-deh-DPDI network.

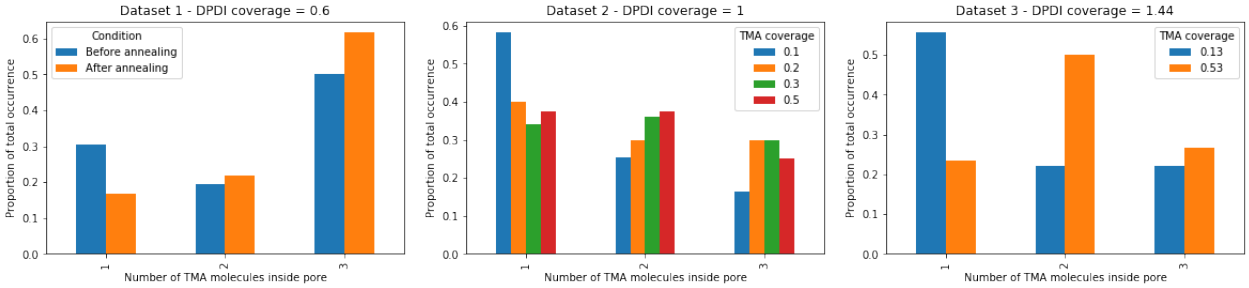

(a) *(b)* *(c)*

Figure 11: *Occurrence of either one, two or three TMA molecules inside the pores of the network for all datasets, thus different DPDI coverages. Figure 11a shows dataset 1: DPDI coverage of 0.6 Å and a TMA coverage of 0.3 Å. This sample is imaged both before and after annealing at 150 °C. Figure 11b shows dataset 2: DPDI coverage of 1 Å and a TMA coverage ranging from 0.1 to 0.5 Å. Figure 11c shows dataset 3: DPDI coverage of 1.44 Å and a TMA coverage of 0.13 and 0.53 Å.*

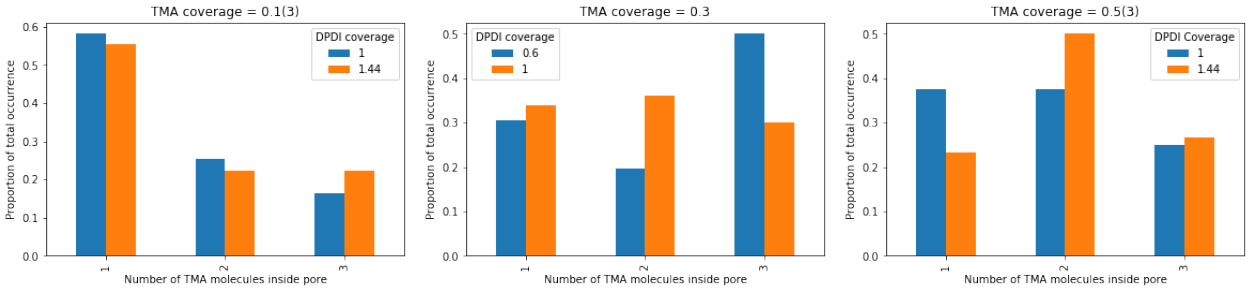

(a) *(b)* *(c)*

Figure 12: *Occurrence of either one, two or three TMA molecules inside the pores of the network for different TMA coverages. Figure 12a shows TMA occurrence for a TMA coverage of 0.1(3) Å and a DPDI coverage of 1 Å and 1.44 Å. Figure 12b shows TMA occurrence for a TMA coverage of 0.3 Å and a DPDI coverage of 0.6 Å (before annealing) and 1 Å. Figure 12c shows TMA occurrence for a TMA coverage of 0.5(3) Å and DPDI coverage of 1 Å and 1.44 Å.*

4.3 Effect of annealing

The sample that has a DPDI coverage of 0.6 Å, was imaged both before and after annealing at 150 °C (423.15K). Figure 13 shows one STM image before annealing, and one after annealing. At first glance it looks like the TMA molecules sit deeper inside the pores after annealing. The bias voltage has the same polarity for both images, so the contrast between the pictures is not a result of this. To check if the TMA molecules indeed sit deeper inside the pore, a height profile is taken of a pore with one, two or three TMA molecules inside it. The height profiles can be found in figure 14. In figure 14a it can be seen that the a single TMA molecule does not sit lower inside the pore after annealing than before annealing. From figures 14b and 14c it can be observed that the TMA molecules indeed sit lower inside the pore after annealing when there are multiple TMA molecules inside the pore. In table 2 the height of the 3-deh-DPDI and TMA molecules relative to the Cu surface are depicted. Also from this it can be observed that the TMA molecules sit lower inside the pore after annealing when there are two or three molecules inside the pore. A possible explanation could be that the surface under the network is restructured. Restructuring of the surface has been observed in for example [21, 22, 23, 24].

Height relative to Cu surface	One TMA inside pore		Two TMA inside pore		Three TMA inside pore	
	Before annealing	After annealing	Before annealing	After annealing	Before annealing	After annealing
3-deh-DPDI	1.3 Å	1.3 Å	1.8 Å	1.4 Å	1.4 Å	1.15 Å
TMA	1.55 Å	1.35 Å	1.25 Å	-0.25 Å	1.25 Å	-0.75 Å

Table 2: *The height of the 3-deh-DPDI molecules and TMA molecules relative to the Cu surface. A positive value means the molecule lies above the Cu surface, whereas a negative value mean it lies below the Cu surface.*

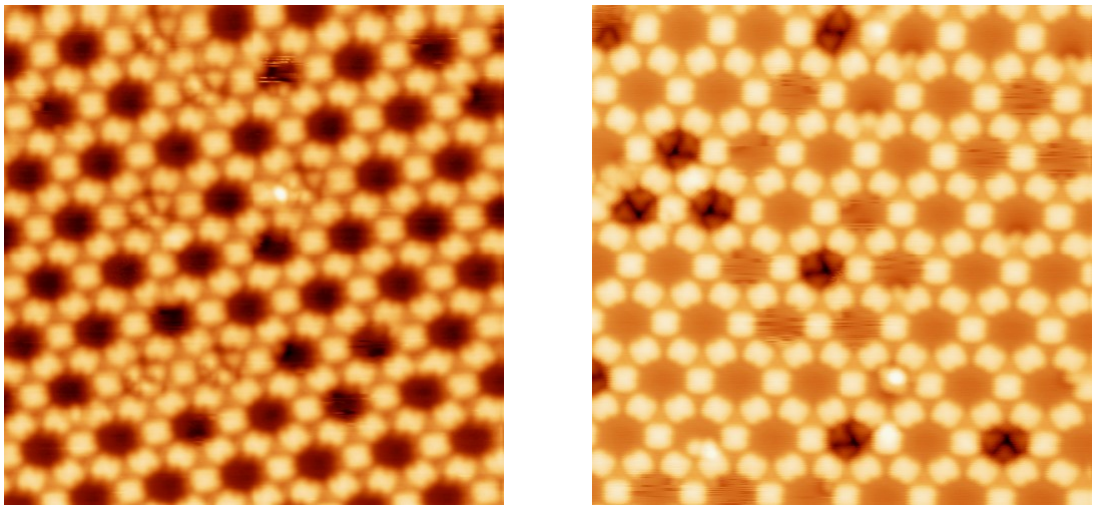

(a) ***(b)***

Figure 13: *STM images of the first sample before and after annealing, DPDI coverage is 0.6 Å and TMA coverage is 0.3 Å. Figure 13a shows the network before annealing (15 nm x 15 nm, U = 1.3 V). Figure 13b shows the network after annealing at 150 °C (15 nm x 15 nm, U = 0.9V).*

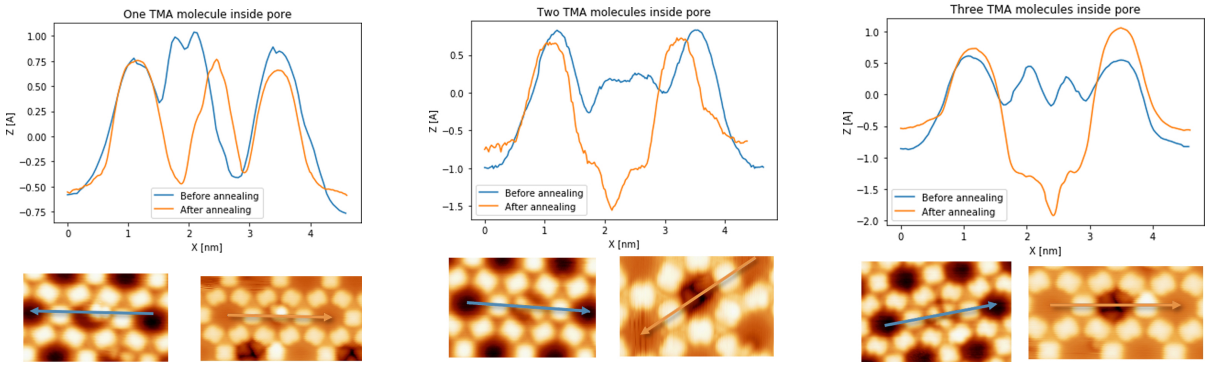

(a) ***(b)*** ***(c)***

Figure 14: *The height profiles for a pore with one, two or three molecule(s) inside the pore. The figure shows the height profiles together with the STM images they were taken from, before (left) and after annealing (right). Figure 14a shows the height profiles of a pore with one TMA molecule inside. Left: (5.5 nm x 3.4 nm, U = -0.9 V), right: (7.3 nm x 3.9 nm, U = 0.9 V). Figure 14b shows the height profiles of a pore with two TMA molecules inside. Left: (5.6 nm x 3.8 nm, U = -1.5 V), right: (50 nm x 32 nm, U = 0.3 V). Figure 14c shows the height profiles of a pore with three TMA molecules inside. Left: (6.4 nm x 3.4 nm, U = 1.3 V), right: (6.4 nm x 4.1 nm, U = 0.9 V).*

4.4 Molecular models

To determine how the TMA molecules fit inside the pores, several different molecular models were made. In figure 19 (section A.1), three models are depicted showing either one, two or three molecule(s) inside the pore of the 3-deh-DPDI network. In this model the TMA molecules are not deprotonated and coordinate in a tip-to-tip manner. For the single TMA inside the pore (figure 19) it can be seen it is able to configure at the junction of two 3-deh-DPDI molecules, which is also seen on the STM images (figure 9a). In figure 19b the hydrogen bonds between the TMA molecules have a length of 1.8 $\dot{A}$. It can be seen that the TMA molecules fit inside the pore in this configuration. However, it is a tight fit. Three TMA molecules coordinating in a tip-to-tip manner (figure 19c) do not fit inside the pore, because repulsion occurs between the TMA molecules and the 3-deh-DPDI molecules. To check if repulsion occurs the van der Waals surfaces of the molecules are used. There should be at least 2.47 $\dot{A}$ between two hydrogen atoms for the van der Waals surfaces to not overlap. When the surfaces overlap, repulsion between two hydrogen atoms occurs.
It is also possible that the non-deprotonated TMA molecules configure in a side-to-side manner instead of a tip-to-tip manner. A model for non-deprotonated TMA with a side-to-side configuration can be found in figure 20 (section A.1). This configuration seems to fit better inside the pore, as can be seen in figure 20a. There is enough space between the hydrogen atoms of the TMA molecules and the 3-deh-DPDI molecules. A side-to-side configuration does not work for three TMA molecules inside a pore, as can be seen in figure 20b. There is too little space where two adjacent 3-deh-DPDI molecules coordinate with the Cu adatoms and because the hydrogens of the TMA molecules are too close to the hydrogens of the 3-deh-DPDI molecules, repulsion occurs.
TMA is known to (partially) deprotonate at room temperature on a Cu surface (section 2.4). Therefore, several molecular models where (some of) the carboxyl groups are deprotonated were tried. In figure 15 the models for TMA with one or two carboxylate groups are depicted. The single TMA molecule (figure 15a) is still able to configure at a junction. For two TMA molecules inside a pore, see figure 15b, it can be seen that the TMA models now can be rotated so that the side of a TMA molecule points towards a junction between two 3-deh-DPDI molecules. This more closely resembles what is seen in an STM image, as in for example figure 9b. From the STM image it looks like the TMA molecules coordinate in a tip-to-tip manner (see figure 8b for reference) and the sides of the molecules coordinate between the junctions of the 3-deh-DPDI network. It is a close fit.
Figure 15c shows three partially deprotonated TMA molecules inside the pore. The lower two TMA molecules have two carboxylate groups, whereas the top one has one carboxylate group. In this configuration the lower two TMA molecules coordinate in a tip-to-tip manner. This configuration resembles what can be seen on the STM images, before annealing, like the ones in figures 9c and 10b.

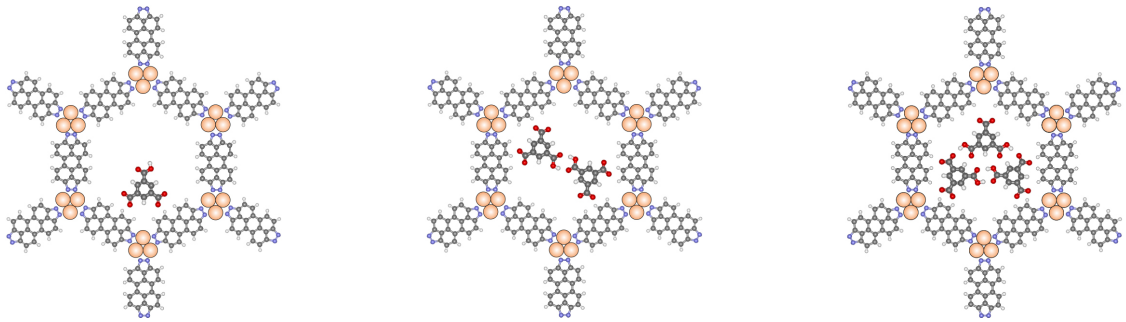

Figure 15: *The molecular models for partially deprotonated TMA inside a pore. Figure 15a shows a single partially deprotonated TMA molecule inside a pore. Figure 15b shows two partially deprotonated TMA molecules inside a pore. Figure 15c shows three partially deprotonated TMA molecules inside a pore where the two bottom TMA molecules coordinate in a tip-to-tip manner.*

It is also possible for the partially deprotonated TMA molecules to coordinate in a side-to-side manner as depicted in figure 16. The model depicted in figure 16a shows two partially deprotonated TMA molecules that interact in a side-to-side manner. The molecules fit in the pore and there is no repulsion between the TMA molecules and 3-deh-DPDI molecules. This configuration does closely resemble what can be seen in the STM image depicted in figure 13b. In the top middle of the STM image a pore with two TMA molecules can be seen, where the TMA molecules seem to interact in a side-to-side manner. Figure 8b, that shows the STM images from the work by *Classen et al.*, can be used as reference. In figure 16b three TMA molecules that interact in a side-to-side manner can be seen. The molecules do not really fit inside the pore, but it should be noted that also this resembles what can be seen on the STM images after annealing as in figure 13b.
It is also possible that the TMA molecules are fully deprotonated, see section 2.4. Therefore, several models with fully deprotonated TMA molecules were tried. When fully deprotonated, the TMA molecules will be

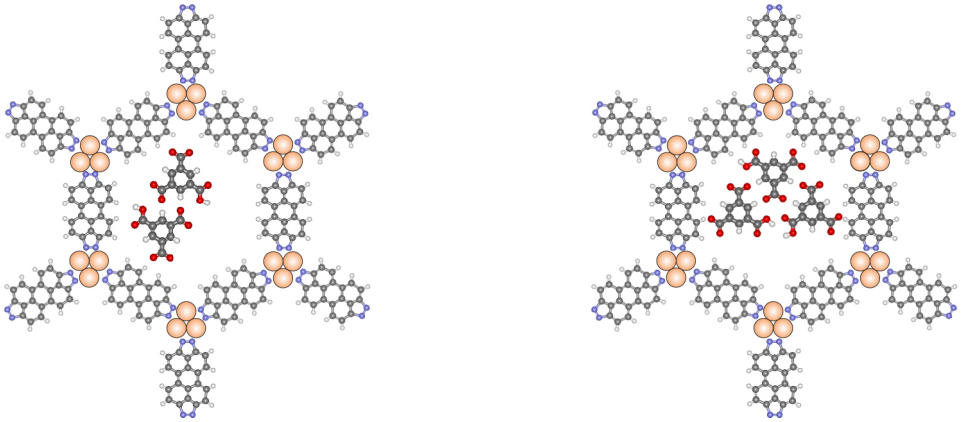

(a) *(b)*

Figure 16: *The molecular models for partially deprotonated TMA inside a pore. The TMA molecules have one carboxyl group and two carboxylate groups. Figure 16a shows two partially deprotonated TMA molecules inside a pore that coordinate in a side-to-side manner. Figure 16b shows three partially deprotonated TMA molecules inside a pore that coordinate in a side-to-side manner.*

referred to as trimesate (TM). A single TM molecule is able to coordinate in a junction of the 3-deh-DPDI network. This closely resembles what is seen on the STM images, like figures 9a and 13b. In figure 17b two TM molecules coordinate to a Cu adatom with two carboxylate groups pointing towards each other. By *Doyle et al.* it is reported that a typical bond length between the oxygen of a carboxylate group and a Cu atom is 1.9 to 2.2 $\dot{A}$ [25]. The bond length between the oxygens and Cu adatom in the model is 2 $\dot{A}$. Furthermore, this configuration closely resembles what is seen on the STM images before annealing (figure 9b). In figure 17c a model for three TM molecules inside the pore is depicted. This model is based on what is seen in the STM images before annealing, like in figure 13a. From the STM images it can be seen that one TM molecule coordinates between two 3-deh-DPDI molecules and two other seem to coordinate with their tips towards each other. Because the TM molecules are fully deprotonated, thus not able to form hydrogen bonds, this is only possible if they coordinate to a Cu adatom. For this model it also applies that the oxygen-adatom distance and the hydrogen bond lengths are in the expected range.

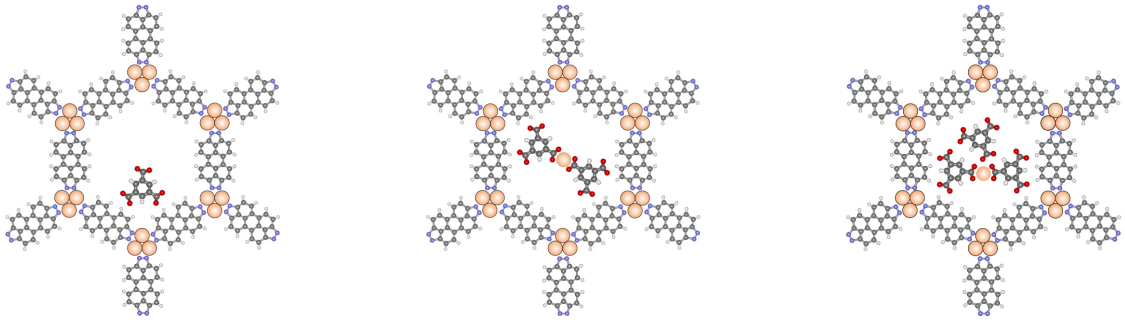

(a) *(b)* *(c)*

Figure 17: *The molecular models for TM inside the pores of the network. The TM molecules have three carboxylate groups. Figure 17a shows a single TM molecule inside a pore. Figure 17b shows two TM molecules inside a pore, where the TM molecules coordinate in a tip-to-tip manner with a Cu adatom. Figure 17c shows three TM molecules inside a pore.*

It is also possible for TM molecules to coordinate in a side-to-side manner. In figure 18a two TM molecules that coordinate in a side-to-side manner can be seen. The hydrogen bond length is of expected length both between the TM molecules and between TM and 3-deh-DPDI molecules. Furthermore, this model closely resembles what is seen on the STM images after annealing (figure 13b, top middle). In figure 18b a model that is based on what is seen in the STM images after annealing (figure 13b) is depicted. In this model the TM molecules coordinate in a side-to-side manner, where the bottom two TM molecules coordinate together with a Cu adatom. Because the TMA molecules are deposited at room temperature it is possible they are fully deprotonated and therefore these models (figures 17 and 18) are most likely to give a representation of the STM images. Furthermore these models fit well in the pores, because both the Cu-O distance as well as the hydrogen bonds are of the expected length and no repulsion between the TM molecules and 3-deh-DPDI molecules occurs. However, to be able to

conclude if the TMA molecules are fully deprotonated, additional data like X-ray photoelectron spectroscopy (XPS) measurements would be needed. The O1s peaks of C−OH and C=O have a different binding energy in the XPS plot. If they are equally present, the TMA molecules are not deprotonated. If the ratio shifts towards C=O, there is deprotonation of the carboxyl groups of TMA.

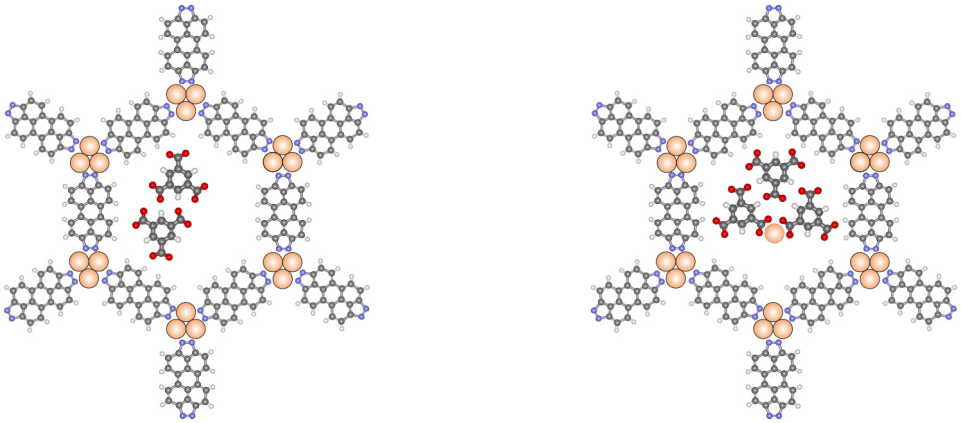

(a) *(b)*

Figure 18: *The molecular models for TM inside the pores of the network. The TM molecules have three carboxyl groups. Figure 18a shows two TM molecules that coordinate side-to-side. Figure 18b shows three TM molecules that coordinate side-to-side, where the bottom two coordinate together with a Cu adatom.*

5 Conclusions

The aim of this research was to understand the host-guest interaction of a self-assembled host network in which TMA acted as a guest. For this, STM images of a 3-deh-DPDI network on a Cu(111) surface that hosted TMA molecules were analyzed. In the STM images it could be seen that the TMA molecules sit with either one, two or three molecule(s) inside the pores of the network. The unit cell of the network has lattice parameters $a = 2.3 \pm 0.2\ nm$, $b = 2.2 \pm 0.2\ nm$ and $\theta = 57 \pm 5°$. This unit cell is not in accordance with the unit cell found by *Matena et al.*[14]. It is likely this difference is due to a calibration error of the STM.
It is found that the TMA molecules prefer to sit alone inside a pore when the TMA coverage is low. For higher TMA coverages the TMA molecules show no clear preference. Furthermore for a DPDI coverage of 0.66 $\dot{A}$ and a TMA coverage of 0.3 $\dot{A}$, the TMA molecules prefer to assemble with three TMA molecules inside the pore. This preference increased slightly after annealing the network at 150°C.
The first sample was imaged both before and after annealing at 150 °C. From the height profiles that were taken, as well as the images, it can be seen that the TMA molecules sit deeper inside the pore after annealing when there are two or three molecules inside the pore. The TMA molecules sit higher above the Cu surface before annealing than after annealing. We do not (yet) understood how the TMA molecules are able to sit lower inside the pore. An explanation for this could be that the molecule-surface interaction is very strong, resulting in the removal of Cu atoms from the surface inside the pore. Because of the removal of the Cu atoms, the TMA is able to sit lower inside the pore. This behavior has, to our knowledge, not been reported in literature yet. Some examples of restructuring of substrates can be found in [21, 22, 23, 24].
Regarding the molecular model, it is likely that the TMA molecules are fully deprotonated. Deprotonation of TMA on Cu surfaces has been found at room temperature before [10, 18]. This is due the strong interaction of the substrate with the molecules. The Cu surface catalyses the deprotonation of the TMA molecules. In addition to this, the models where the TMA molecules are fully deprotonated show the best fit inside the pores and have the least repulsion with the 3-deh-DPDI molecules. In these models, the TMA molecules coordinate together with Cu adatoms which have diffused from the step edges of the surface. In total, five different models are proposed; where the TMA molecules coordinate in a tip-to-tip manner before annealing and in a side-to-side manner after annealing the network. These models are pictured in figures 17 and 18. However, that the TMA molecules are fully deprotonated cannot be said without certainty unless additional data like XPS measurements is considered.
For future research on this host-guest network, the influence of the DPDI coverage (and TMA coverage) on the occurrence of TMA could be investigated by trying more different DPDI coverages with equal TMA coverages, and vice versa. Furthermore, to see if the occupation of the pores increases with increasing TMA coverage one could look into the total amount of pores that are occupied and compare this to the total amount of pores that are left without TMA molecules. To conclude if the TMA molecules are fully deprotonated one could perform

XPS measurements on the network.

6 Acknowledgements

I would like to thank my supervisor Meike Stöhr for letting me do this project within the Surface Science group and the help she has offered me. I would also like to thank the members of the Surface Science group for their insights and help. A special thank you must go to Mihaela Enache, for her daily supervision and all the help and support she offered.

7 References

[1] Nobel Media AB 2020, "The nobel prize in chemistry 1987." [Online]. Available: https://www.nobelprize.org/prizes/chemistry/1987/press-release/

[2] S. Jasty, "Introduction to molecular self-assembly," *Sigma-Aldrich Material Matters*, vol. 1, no. 3, 2006.

[3] G. M. Whitesides, J. P. Mathias, and C. T. Seto, "Molecular self-assembly and nanochemistry: a chemical strategy for the synthesis of nanostructures," *Science*, vol. 254, no. 5036, pp. 1312–1319, 1991.

[4] A. Kühnle, "Self-assembly of organic molecules at metal surfaces," *Current Opinion in Colloid & Interface Science*, vol. 14, no. 2, pp. 157–168, 2009.

[5] J. Teyssandier, S. De Feyter, and K. S. Mali, "Host–guest chemistry in two-dimensional supramolecular networks," *Chemical Communications*, vol. 52, no. 77, pp. 11 465–11 487, 2016.

[6] M. Schmid, "Schematic representation of scanning tunneling microscope," Apr 2020, [Accessed June 8 2020]. [Online]. Available: https://commons.wikimedia.org/wiki/File:Scanning_Tunneling_Microscope_schematic.svg

[7] C. J. Chen, *Introduction to scanning tunneling microscopy*. Oxford University Press on Demand, 1993, vol. 4.

[8] J. Li, S. Gottardi, L. Solianyk, J. C. Moreno-Lopez, and M. Stohr, "1, 3, 5-benzenetribenzoic acid on cu (111) and graphene/cu (111): A comparative stm study," *The Journal of Physical Chemistry C*, vol. 120, no. 32, pp. 18 093–18 098, 2016.

[9] A. Dmitriev, N. Lin, J. Weckesser, J. Barth, and K. Kern, "Supramolecular assemblies of trimesic acid on a cu (100) surface," *The Journal of Physical Chemistry B*, vol. 106, no. 27, pp. 6907–6912, 2002.

[10] T. Classen, M. Lingenfelder, Y. Wang, R. Chopra, C. Virojanadara, U. Starke, G. Costantini, G. Fratesi, S. Fabris, S. De Gironcoli *et al.*, "Hydrogen and coordination bonding supramolecular structures of trimesic acid on cu (110)," *The Journal of Physical Chemistry A*, vol. 111, no. 49, pp. 12 589–12 603, 2007.

[11] M. S. Baviloliaei and L. Diekhöner, "Molecular self-assembly at nanometer scale modulated surfaces: trimesic acid on ag (111), cu (111) and ag/cu (111)," *Physical Chemistry Chemical Physics*, vol. 16, no. 23, pp. 11 265–11 269, 2014.

[12] S. J. Griessl, M. Lackinger, F. Jamitzky, T. Markert, M. Hietschold, and W. M. Heckl, "Room-temperature scanning tunneling microscopy manipulation of single c60 molecules at the liquid- solid interface: playing nanosoccer," *The Journal of Physical Chemistry B*, vol. 108, no. 31, pp. 11 556–11 560, 2004.

[13] C. Kittel *et al.*, *Introduction to solid state physics*. Wiley New York, 1976, vol. 8.

[14] M. Matena, J. Björk, M. Wahl, T.-L. Lee, J. Zegenhagen, L. H. Gade, T. A. Jung, M. Persson, and M. Stöhr, "On-surface synthesis of a two-dimensional porous coordination network: Unraveling adsorbate interactions," *Physical Review B*, vol. 90, no. 12, p. 125408, 2014.

[15] M. Stöhr, M. Wahl, H. Spillmann, L. H. Gade, and T. A. Jung, "Lateral manipulation for the positioning of molecular guests within the confinements of a highly stable self-assembled organic surface network," *Small*, vol. 3, no. 8, pp. 1336–1340, 2007.

[16] J. Ubink, M. Enache, and M. Stöhr, "Bias-induced conformational switching of supramolecular networks of trimesic acid at the solid-liquid interface," *The Journal of Chemical Physics*, vol. 148, no. 17, p. 174703, 2018.

[17] N. Lin, D. Payer, A. Dmitriev, T. Strunskus, C. Wöll, J. V. Barth, and K. Kern, "Two-dimensional adatom gas bestowing dynamic heterogeneity on surfaces," *Angewandte Chemie International Edition*, vol. 44, pp. 1488–1491, 2005.

[18] N. Lin, A. Dmitriev, J. Weckesser, J. V. Barth, and K. Kern, "Real-time single-molecule imaging of the formation and dynamics of coordination compounds," *Angewandte Chemie International Edition*, vol. 41, no. 24, pp. 4779–4783, 2002.

[19] I. Horcas, R. Fernández, J. Gomez-Rodriguez, J. Colchero, J. Gómez-Herrero, and A. Baro, "Wsxm: a software for scanning probe microscopy and a tool for nanotechnology," *Review of Scientific Instruments*, vol. 78, no. 1, p. 013705, 2007.

[20] J. C. Vickerman and I. S. Gilmore, *Surface analysis: the principal techniques.* John Wiley & Sons, 2011.

[21] M. Gabriel, M. Stöhr, R. MöllerRID *et al.*, "Growth of 3, 4, 9, 10-perylenetetracarboxylic-dianhydride (ptcda) on cu (110) studied by stm," *Applied Physics A*, vol. 74, no. 2, pp. 303–305, 2002.

[22] M. Stöhr, M. Gabriel, and R. Möller, "Investigation of the growth of ptcda on cu (110): an stm study," *Surface science*, vol. 507, pp. 330–334, 2002.

[23] P. Murray, M. Pedersen, E. Lægsgaard, I. Stensgaard, and F. Besenbacher, "Growth of c 60 on cu (110) and ni (110) surfaces: C 60-induced interfacial roughening," *Physical Review B*, vol. 55, no. 15, p. 9360, 1997.

[24] H. Li, K. Pussi, K. Hanna, L.-L. Wang, D. D. Johnson, H.-P. Cheng, H. Shin, S. Curtarolo, W. Moritz, J. Smerdon *et al.*, "Surface geometry of c 60 on ag (111)," *Physical review letters*, vol. 103, no. 5, p. 056101, 2009.

[25] A. Doyle, J. Felcman, M. T. do Prado Gambardella, C. N. Verani, and M. L. B. Tristão, "Anhydrous copper (ii) hexanoate from cuprous and cupric oxides. the crystal and molecular structure of cu2 (o2cc5h11) 4," *Polyhedron*, vol. 19, no. 26-27, pp. 2621–2627, 2000.

A Appendix

A.1 Molecular models

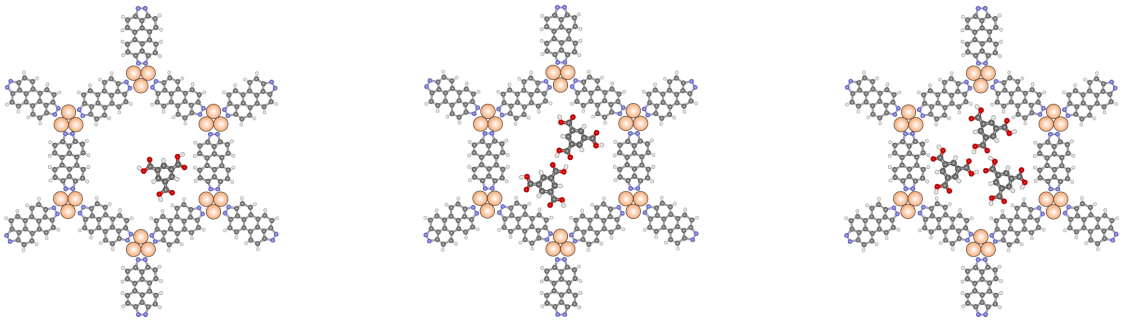

(a) ***(b)*** ***(c)***

Figure 19: *The molecular models for TMA molecules inside a pore. The TMA molecules are not deprotonated and coordinate in a tip-to-tip manner in all three models. Figure 19a shows a singular TMA molecule inside a pore. Figure 19b shows two TMA molecules inside a pore where the molecules coordinate tip-to-tip. Figure 19c shows three TMA molecules inside a pore where the molecules coordinate tip-to-tip.*

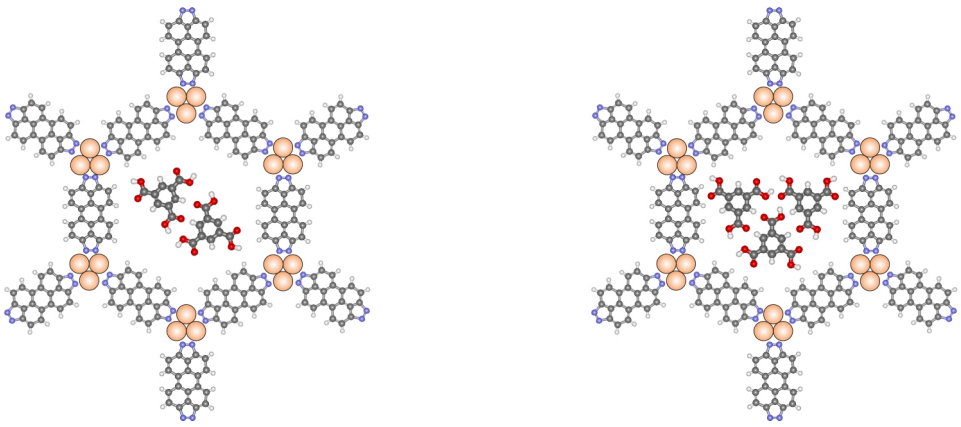

(a) *(b)*

Figure 20: *The molecular models for TMA molecules inside a pore, where the TMA molecules coordinate in a side-to-side manner. Figure 20a shows two TMA molecules coordinating in a side-to-side manner. Figure 20b shows three TMA molecules coordinating in a side-to-side manner.*